Journal of Electrical Engineering, Vol. 75, No. 1, 2024, pp. 14-23

sciendo

PAPERS

Harnessing XPM effects in non-linear directional couplers for 4-bit gray code conversion and even parity verification

Ajay Yadav[1], Ajay Kumar[2], Amit Prakash[3]

The all-optical switching phenomena in the non-linear directional coupler using cross-phase modulation (XPM) effect have been proposed. It is designed to generate an all-optical XOR functionality, considering the XOR logic gates as a basic module the design and analysis of an efficient all-optical 4-bit binary to gray code converter and 4-bit even parity checker circuit is proposed. The design methodology includes the switching of a weak continuous-wave (CW) signal, which is controlled by the combination of two controlled pump signals. In this paper, mathematical analysis of the coupled mode theory associated with optical directional couplers has been discussed. The switching characteristics of XPM effect based All-optical directional couplers have been examined for appropriate values of the controlled pump signals. Appropriate values of extinction ratio and corresponding controlled pump signal levels are investigated for an efficient generation of XOR logic gates. Further, the detailed analysis of layout generation and design aspects of All-optical 4-bit binary to gray code converter and 4-bit even parity checker circuits have been carried out. The proposed methodology is verified by the appropriate simulation results, which include the transmittivity, extinction ratio (Xratio) curve variation and dynamic time domain plot associated with proposed units.

Keywords: nonlinear directional coupler, cross-phase modulation, optical switching, gray code converter, even parity checker

1 Introduction

Optical fiber communication has emerged as a pivotal technological advancement in the telecommunication industry, with ongoing research and trials demonstrating its technical feasibility and potential for transforming communication technology. The economic viability of fiber networks in various applications compared to existing systems will likely dictate its impact on the communication industry. To meet the increasing demand for high-speed communications, researchers are replacing traditional electrical components with optical switching components, utilizing fundamental building blocks such as AND, OR, NOT, XOR, and XNOR logic gates. A variety of devices, including the Mach-Zehnder Interferometer (MZI) [1], Micro-ring Resonator (MRR) [2], Surface Plasmon Resonance (SPR) [3], Fiber Bragg grating (FBG) [4], Photonic Crystal Waveguide (PCW) [5], and Directional Coupler [6-11], are available for constructing All-optical logic gates and switches. Photonic switching involves manipulating optical signals between different modes, relying on the intensity-dependent dynamics of the optical beam. Self-phase modulation (SPM) and cross-phase modulation (XPM) have emerged as essential nonlinear optical effects for ultrafast switching within femtoseconds [12].

Nonlinear optics extends beyond fiber-based applications and can be applied to various types of waveguides through strategic design and fabrication. The implementation of XPM-based nonlinear directional coupler switching has been introduced for the design of complex systems such as the 4-bit All-optical gray code converter and even parity checker [13-16]. The asymmetric nonlinear directional coupler serves as a versatile platform for an array of logic gates and devices, presenting significant potential for high-speed operations in sequential and combinational circuits. The intricate mechanics underlying these All-optical photonic crystal logic gates underscore their role in facilitating high-speed and energy-efficient photonic computation through nonlinear directional couplers [17]. Additionally, the investigation of directional couplers with unequal nonlinearity distributions has garnered attention for its intriguing dynamics and unique properties by leveraging analogous directional couplers, digital optical switches can be developed, offering avenues for enhancing optical switching capabilities [18]. An all-optical method for fundamental logic gates using nonlinear optical fiber couplers, optical switching, and improved bistability in an asymmetric coupler with metamaterial, and comparative review on all-optical logic gate design for ultrafast switching These advancements contribute to the technological progress

Fiber Optics Laboratory, National Institute of Technology Jamshedpur, Jharkhand, India, 831014
[1] ajayyadavnitjsr@gmail.com, [2] ajay.ece@nitjsr.ac.in, [3] amitprakash.ece@nitjsr.ac.in

https://doi.org/10.2478/jee-2024-0003, Print (till 2015) ISSN 1335-3632, On-line ISSN 1339-309X

of optical communication and switching systems over conventional methods [19-21].

This study primarily focuses on enhancing the utilization of optical directional couplers as an optical switch, emphasizing their significant impact on dense Wavelength Division Multiplexing (WDM). The subsequent sections provide a comprehensive overview of the underlying methodology, mathematical descriptions, and simulation results pertaining to the design and implementation of optical directional couplers for various applications [22]. By shedding light on the innovative capabilities of these couplers, the research underscores the transformative potential of optical fiber communication and nonlinear optics in revolutionizing the telecommunications landscape.

The primary scientific contributions of this work are the proposal and investigation of an all-optical XOR functionality based on the XPM effect employing a nonlinear directional coupler to design the proposed circuit. We propose the design and analysis of an efficient all-optical 4-bit binary to gray code converter and a 4-bit even parity checker circuit based on this approach. The novel design technique utilizes the controlled mixing of two pump signals to manipulate a CW signal. This study adds to the body of knowledge by doing a thorough mathematical analysis of the coupled mode theory associated with optical directional couplers and investigating the switching properties of XPM effect-based all-optical directional couplers. A notable contribution of our study is finding optimal values for the regulated pump signals, extinction ratio, and their influence on the efficient creation of proposed optical circuits. Furthermore, the complete examination of layout generation and design features, proven by simulation results such as transmittivity, Xratio curve change, and dynamic time domain plots, substantiates the suggested feasibility of the proposed methodology.

2 XPM-induced switching in directional couplers

A coupler is a significant optical device that may perform a variety of functions such as switching, sensing, and routing. It enables light to be transmitted from one waveguide to another, making it suitable for a variety of applications. The directional coupler is typically associated with two input and two output ports, as shown in Fig. 1. Coupled mode theory is a fundamental concept in optical waveguide systems, including directional couplers. It provides a theoretical framework for understanding the interactions between different guided modes in coupled waveguides. In the context of XPM effect-based optical directional couplers, coupled mode theory becomes essential to describe the dynamic coupling and switching behaviour between modes, shedding light on the underlying mechanisms controlling the switching activity.

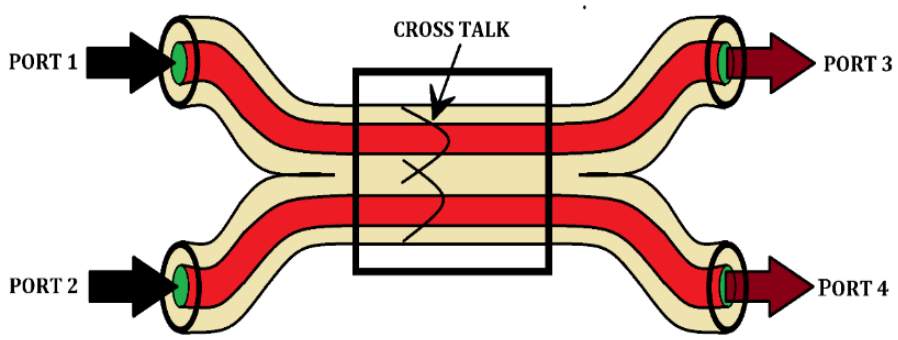

Fig. 1. Layout digram of the optical directional coupler

The coupled mode theory equations are utilized to illustrate the fundamental concept of optical directional couplers. The simpler form of the equation can be represented as follows:

$$\frac{dA}{dz} \; i\kappa_{11}A(z) \; + \; i\kappa_{12}B(z)e^{i\Delta\beta z} \qquad (1)$$

and similarly

$$\frac{dB}{dz} = \; i\kappa_{21}A(z)e^{-i\Delta\beta z} \; + \; i\kappa_{22}B(z), \qquad (2)$$

where $\Delta\beta = (\beta_2 \; - \; \beta_1)$.

Equations for the evolution of amplitude are $A(z)$ and $B(z)$. Equations (1) and (2) are coupled equation, i.e., the variation of A depends upon B and vice-versa through the coupling terms.

It holds

$$\frac{P_1(z)}{P_0} \; = \; 1 \; - \left(\frac{\kappa^2}{\gamma^2}\right)\sin^2(\gamma z). \qquad (3)$$

Here, P_1 represents the input high-power pump light signal with power P_1. P_0 is the total power through the two ports, thus $P_0 = P_1(z) + P_2(z)$. As z increases, $P_1(z)/P_0$ varies sinusoidally, hence after a certain length the switching phenomenon takes place. If there is no loss, the total power remains conserved, i.e., the total power

$$P_T = P_1(z) + P_2(z) = P_0$$

and

$$\frac{P_2(z)}{P_0} = \frac{\kappa^2}{\gamma^2}\sin^2(\gamma z). \tag{4}$$

From Eqns. (3) and (4), the shifting of power is taking place sinusoidally. Figure 2 represents the basic module of the directional coupler based on the XPM effect.

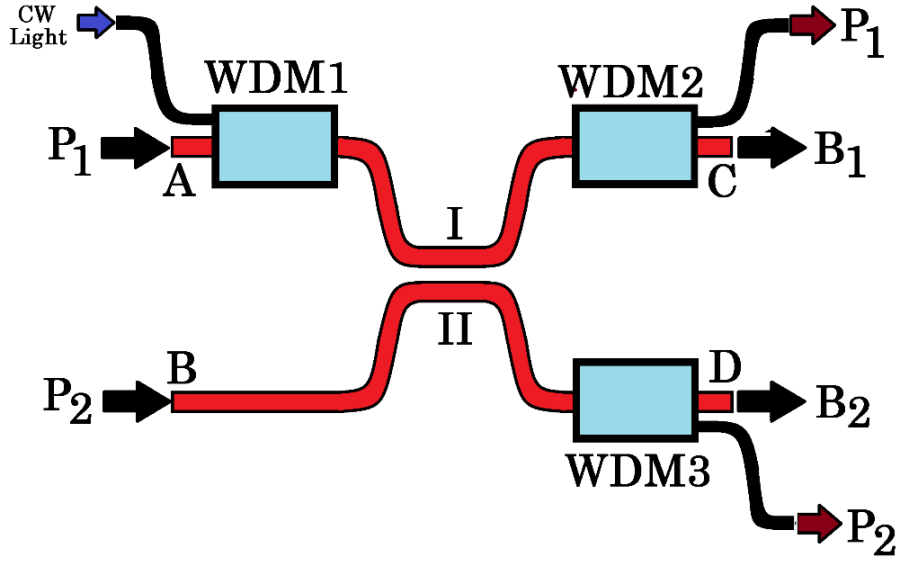

Fig. 2. XPM effect based directional couplers generating the switching phenomena

The XPM is observed in core I and II due to the Kerr effect in such a manner that the symmetric coupler changes into an asymmetric coupler. The coupled equation of the coupler can be represented based on the coupled non-linear Schrödinger wave equations neglecting the time related terms as in equations (5) and (6).

$$\frac{dA_1}{dz} = i\kappa_{12}A_2 + i\beta_1 A_1 + 2i\gamma P_1 A_1 \tag{5}$$

$$\frac{dA_2}{dz} = i\kappa_{21}A_1 + i\beta_2 A_2 + 2i\gamma P_2 A_2 \tag{6}$$

Here, β_1 and β_2 are propagation constants for channels I and II, κ_{12} and κ_{21} are coupling parameters. Now, taking $A_1 = B_1 e^{i(\beta_1+\beta_2)z/2}$, $A_2 = B_2 e^{i(\beta_1+\beta_2)z/2}$, after substitution in Eqns. (5) and (6), equations can be written as:

$$\frac{dB_1 e^{i(\beta_1+\beta_2)z/2}}{dz} =$$
$$= i\kappa_{12}B_2 e^{i(\beta_1+\beta_2)z/2} + i\beta_1 B_1 e^{i(\beta_1+\beta_2)z/2} +$$
$$+2i\gamma P_1 A_1 B_1 e^{i(\beta_1+\beta_2)z/2}$$

$$e^{i(\beta_1+\beta_2)z/2}\frac{dB_1}{dz} + B_1 i\frac{(\beta_1+\beta_2)}{2}\left(e^{i(\beta_1+\beta_2)z/2}\right) =$$
$$= i\kappa_{12}B_2 e^{i(\beta_1+\beta_2)z/2} + i\beta_1 B_1 e^{i(\beta_1+\beta_2)z/2} +$$
$$+2i\gamma P_1 A_1 B_1 e^{i(\beta_1+\beta_2)z/2}$$

$$\frac{dB_1}{dz} = i\kappa B_2 + i\zeta_1 B_1 \tag{7}$$

where $\kappa_{12} = \kappa$, and $\zeta_1 = 2\gamma P_1 + \frac{(\beta_1-\beta_2)}{2}$.

Equation (6) can be transformed and represented as

$$\frac{dB_2}{dz} = i\kappa B_1 + i\zeta_2 B_2 \tag{8}$$

where $\kappa_{12} = \kappa$, and $\zeta_2 = 2\gamma P_1 - \frac{(\beta_1-\beta_2)}{2}$.

Solving Eqns. (7) and (8) on applying suitable boundary conditions $B_1(z=0)=B_{10}$ and $B_2(z=0)=B_{20}$ yields

$$B_1(z) = e^{-i\kappa_1 z} \times$$
$$\times\left[B_{10}\cos(\kappa_2 z) + i\left(\frac{\gamma(P_1 - P_2)}{\kappa_2}B_{10} + \frac{\kappa}{\kappa_2}B_{20}\right)\sin(\kappa_2 z)\right] \tag{9}$$

$$B_2(z) = e^{-i\kappa_1 z} \times \\ \times \left[B_{20}\cos(\kappa_2 z) - i\left(\frac{\gamma(P_1 - P_2)}{\kappa_2} B_{20} + \frac{\kappa}{\kappa_2} B_{10}\right)\sin(\kappa_2 z)\right] \tag{10}$$

where
$\kappa_1 = \gamma(P_1 + P_2)$ and $\kappa_2 = [\gamma^2(P_1 - P_2)^2 + \kappa^2]^{1/2}$ with approximation $\Delta\beta = 0$.

The extinction ratio can be used to analyse the switching activity. The extinction ratio for the on-off switch should be as high as possible for the perfect switching. The extinction ratio is

$$X_{ij} = \frac{\int_{-\infty}^{\infty} |B_i|^2 dt}{\int_{-\infty}^{\infty} |B_j|^2 dt}, \tag{11}$$

where $(i, j = 1, 2)$.

The switching performance can be checked using transmission function

$$T_i = \frac{\int_{-\infty}^{\infty} |B_i|^2 dt}{\int_{-\infty}^{\infty} |B_{10}|^2 dt}, \tag{12}$$

where $(i, j = 1, 2)$.

The arms of the directional coupler are made of an optical fiber based on Bi_2O_3 that has strong nonlinearity, which is measured by a nonlinear coefficient $\gamma = 1360\ \mathrm{W^{-1}km^{-1}}$ [13]. The device coupling coefficient is $\kappa = 5\ \mathrm{m^{-1}}$, and the appropriate coupling length is $L = \pi/2\kappa$, P_1 is adjustable from 0 to 30 W. P_1 and P_2 have a wavelength of 980 nm, while the weak CW light has a wavelength of 1550 nm. Figure 3 illustrates the transmission as a function of P_1 and P_2, which can be calculated using Eqn. (12). Pump P_1 inputs from port A as shown in Fig. 3a, while WDM adds a low CW light to the port A and port B has no input. The Kerr effect and XPM will be produced in the directional coupler when the power of pump P_1 is increased. The output route is clearly altered when the pump power P_1 attains 2.8 W which is the threshold power (P_{th}) [12].

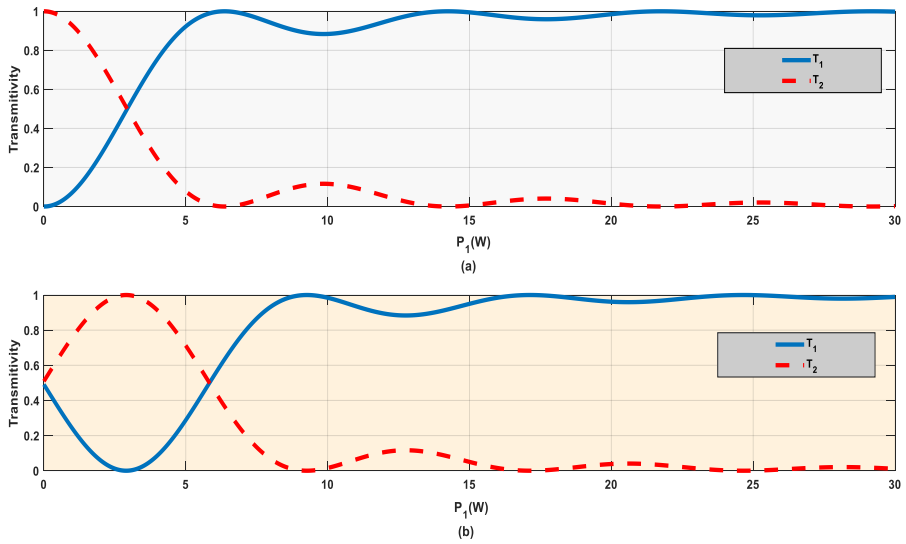

Fig. 3. Switching characteristics of transmission as a function of P_1 when (a) $P_2 = 0$ W (b) $P_2 = 2.8$ W.

In Fig. 3b, a pump signal P_1 and a weak CW light are added to channel I, there is no CW light input in port B, and pump signal $P_1 = 2.8$ W is provided as an input. Due to the difference in wavelength between the pump signal and the weak CW light signal, the pump P_1 and P_2 remains in channel I and II, respectively. Two pumps execute XPM for CW light in cores I and II, respectively. For $P_1 = 0\ \mathrm{W}, P_2 = 2.8\ \mathrm{W}$ and $P_1 = 5.8\ \mathrm{W}, P_2 = 2.8\ \mathrm{W}$, as observed in Fig. 3b, the splitting ratio reaches1:1 due to the evanescent coupling and XPM. When $0 < P_1 < 2.8$ occurs, the majority of the weak CW light signal power is transferred to core II. When $P_1 > 2.8$ W, the weak CW light will move to core I as P_1 increases. When $P_1 = P_2 = 2.8$ W, two pump signal in core I and core II conduct XPM on the CW light, and a fiber coupler with $L = \pi/2\kappa$ transmits all of the CW light power to the core II, as shown in Fig. 3b. Further, by varying the power of P_1 and P_2 an alternative logic gates can be designed.

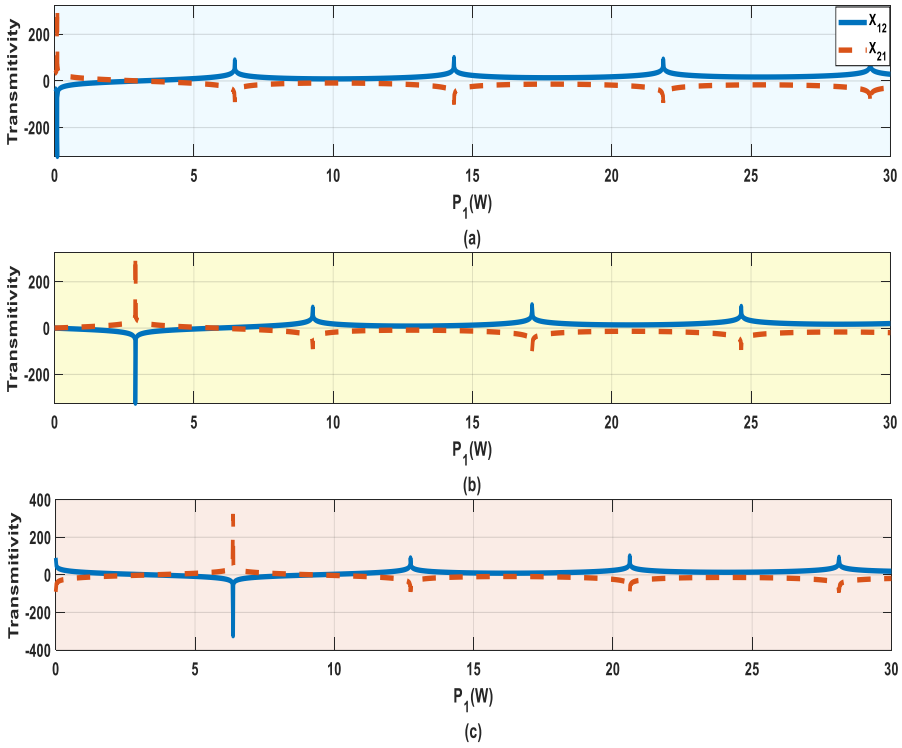

Fig. 4. Xratio level characteristics as a function of P_1 when (a) $P_2 = 0$ W, (b) $P_2 = 2.8$ W, (c) $P_2 = 6.3$ W

Figure 4a depicts the Xratio level as a function of pump power is calculated using equation (11). Initially, $B_{10} = 1$ mW, $B_{20} = 0$, and $P_2 = 0$ is assumed. The optical switching action can be achieved if $P_1 > P_{th}$. In Fig. 4.a, a pump signal is given in port A which flows through fiber core I with XPM, whereas the SPM is in the fiber core II. When $P_1 = 0$ and Xratio_{21} is set to maximum 324.3 dB, the fiber coupler sends all weak CW light power to the core II. The $\text{Xratio}_{12} < 0$ when $P_1 < 2.8$ W and $\text{Xratio}_{12} > 0$ when $P_1 > 2.8$ W. This signifies that the pump signal reverses the switching and returns the weak CW light to the first channel.

Figure 4b shows the plot of Xratio function as P_1 when $B_{10} = 1$ mW, $B_{20} = 0$, and $P_2 = 2.8$ W. When $P_1 = 0$, and $P_2 = 2.8$ W, which is less than the P_{th}, the $\text{Xratio}_{12} = -0.555$ dB and $\text{Xratio}_{21} = 0.555$ dB. Due to XPM, the Xratio tends to be zero when $P_1 = 0$, similar as shown in Fig. 4.a, when $P_1 = 2.8$ W. In Fig. 4b, when $P_1 = P_2 = 2.8$ W, two pumps conduct XPM on the CW light in core I and II, and all power of weak CW light is transferred to the core II. The $\text{Xratio}_{12} = -337.4$ dB and $\text{Xratio}_{21} = 337.4$ dB. Here $P_2 = 6.3$ W in Fig. 4c, which is greater than P_{th}. When $P_1 = 0$, the weak CW light signal is limited to the same core from which it was launched, and the $\text{Xratio}_{12} = 88.25$ dB and $\text{Xratio}_{21} = -88.25$ dB. When $P_1 = 6.368$ W, as previously described, two pumps execute the XPM to the CW light in core I and core II, respectively. All CW light power transfers to core II, and the Xratio_{21} reaches the maximum of 333.3 dB.

3 All-optical binary to gray code converter

It is interesting to implement the All-optical gray-code conversion techniques using XPM effect in the directional couplers. The layout of the 4-bit all-optical binary-to-gray code converter is shown in Fig. 5, highlighting the vital significance of the XPM effect within the directional coupler. The design and implementation of the layout emphasize the specific arrangement of components and the utilization of the XPM effect in the proper functioning of binary-to-gray code conversion. This layout is constructed using three nonlinear directional couplers based on the XPM effect. The first gray code output (G_1) is obtained from port C_1 when the optical equivalent of binary numbers b_0 and b_1 are sent to port A_1 and B_1 of the first directional coupler (DC1). When binary numbers b_1 and b_2 are sent to the port A_2 and B_2 of the second directional coupler (DC2), a second gray code output (G_2) is obtained from the port C_2. Similarly, the third gray code output (G_3) is obtained from the C_3 port when the binary b_2 and b_3 are fed into port A_3 and B_3 of the third directional coupler (DC3). The fourth gray code output (G_4) is same as binary input b_3.

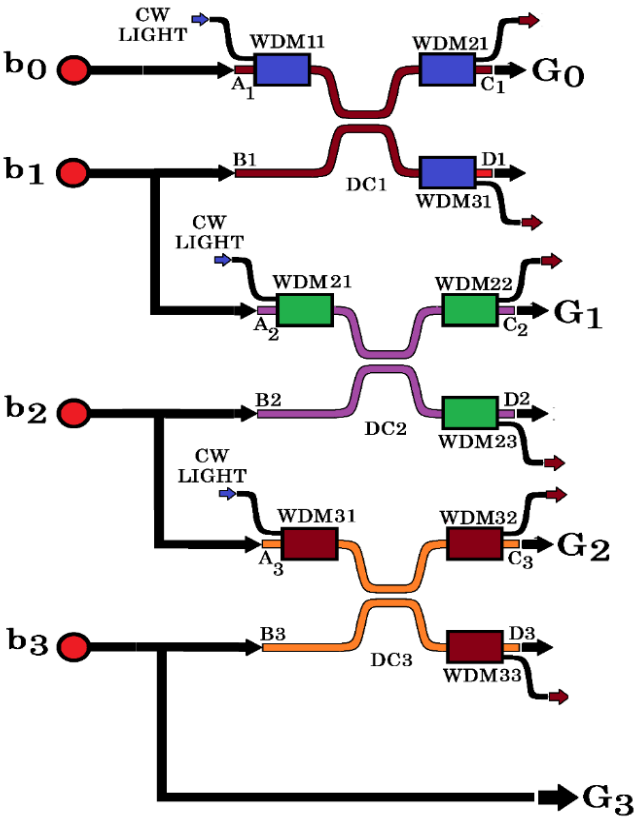

Fig. 5. Layout of 4-bit All-optical binary to gray code converter using XPM effect in the directional coupler

4 Switching mechanism

The switching phenomena of XPM effect based directional coupler as shown in Fig. 2 where logic 1 signifies the existence of a pump signal at input port and logic 0 is the unavailability of the pump signal. For power value *P*=2.8 W the optical logic is 1, whereas *P*=0 for optical logic 0 as shown in Table 1.

Table 1. Optical logic truth table for $P = 2.8$ W

Port A	Port B	X_{12} (dB)	Port C	X_{21} (dB)	Port D
0	0	−337.3	0	337.3	1
0	1	−0.555	1	0.555	1
1	0	−0.555	1	0.555	1
1	1	−320.4	0	320.4	1
$C = A \oplus B$					

Xratio value for the configuration is (0,0), (0,1), (1,0) and (1,1). At (0,0) input, the value of $\text{Xratio}_{12} = -337.4$ dB and $\text{Xratio}_{21} = 337.4$ dB. An optical fiber coupler with coupling length $L = \pi/2\kappa$ sends 100% of CW light power will be transmitted to the second core. The CW light power exists in both ports C and D for (0,1) input and the value of $\text{Xratio}_{12} = -0.555$ dB and $\text{Xratio}_{21} = 0.555$ dB. For (1,0) input it is the same as the (0,1) configuration. For (1,1) input all CW light power will be transmitted to the second core and the value of $\text{Xratio}_{12} = -320.4$ dB and $\text{Xratio}_{21} = 320.4$ dB. Therefore, by using the above technique XOR operation can be established.

The layout of the proposed 4-bit All-optical binary to gray code converter using XPM effect in the directional coupler as shown in Fig. 5 is simulated and the results are shown in Fig. 6 for $P = 6.3$ W. At (0,0) input, the value of $\text{Xratio}_{12} = -340.4$ dB and $\text{Xratio}_{21} = 340.4$ dB. For (0,1) and (1,0) input configurations, the pump signal is greater than the threshold power therefore the weak CW light is limited to the same core from which it was launched. For above input configuration the value of $\text{Xratio}_{12} = 88.25$ dB and $\text{Xratio}_{21} = -88.25$ dB. Further, for (1,1), the $\text{Xratio}_{12} = -340.3$ dB and $\text{Xratio}_{21} = 340.3$ dB. The logic gates $C = A \oplus B$ and $D = \overline{A \oplus B}$ are constructed for the All-optical binary to gray code converter as shown in Fig. 5. It is observed that the wavelength conversion is used to transmit information from pump signal to the weak CW light and that All-optical logic gates based on wavelength conversion has a high switching contrast.

The proposed design of 4-bit All-optical binary to gray converter using the XPM effect is simulated, as shown in Fig. 7. Here, the 1st row represents the input binary data bit pattern $B_0 \rightarrow$ (0101010101010101), which corresponds to the gray code pattern $G_0 \rightarrow$ (0110011001100110) as in 5th row. Further, 2nd row represents the input binary data bit pattern $B_1 \rightarrow$ (0011001100110011), which corresponds to the gray code $G_1 \rightarrow$ (0011110000111100) as in 6th row. The 3rd row represents the input data bit pattern $B_2 \rightarrow$ (0000111100001111), which corresponds to the gray code $G_2 \rightarrow$ (0000111111110000) as in 7th row. Similarly, 4th row represents the input data bit pattern $B_3 \rightarrow$ (0000000011111111), which corresponds to the gray code $G_3 \rightarrow$ (0000000011111111) as in 8th row.

The simulation outcomes are validated using the standard output for 4-bit binary to gray code converter. Therefore, the proposed device specifies an efficient approach to convert a 4-bit binary input data into a 4-bit gray code while operating in the optical domain. Gray code converters are suitable for switching applications. Consequently, the implementation of an optical gray code converter can enhance the performance of switching devices by increasing the switching speed.

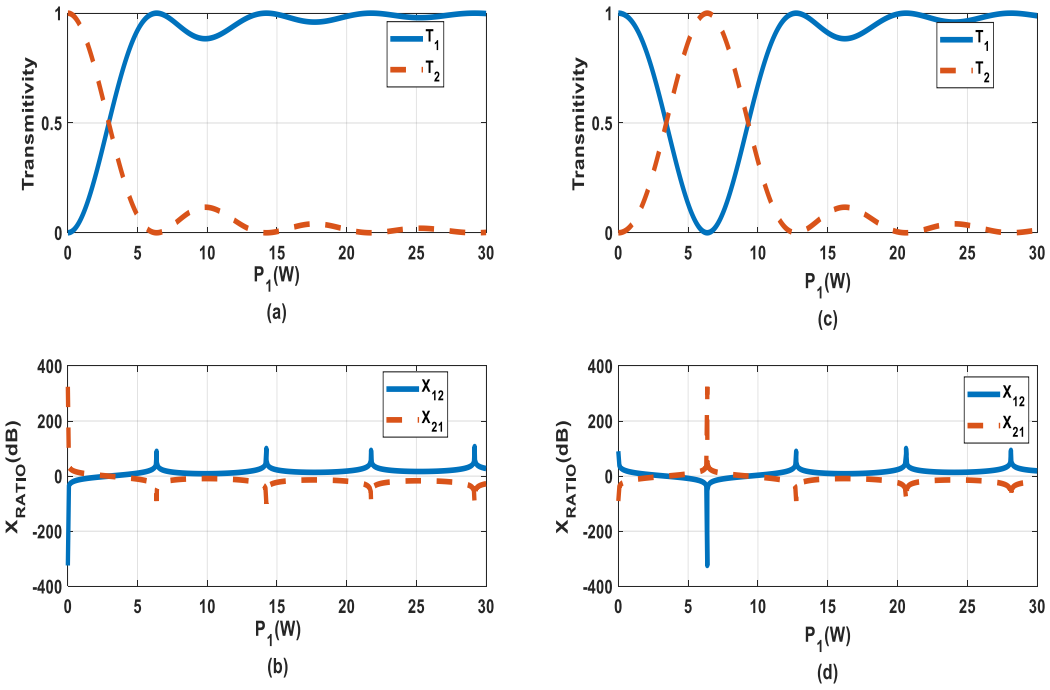

Fig. 6. XOR/XNOR logic gate used in 4-bit binary to gray code converter: (a) Transmittivity curve for $P_2 = 0$ W, (b) Xratio curve for $P_2 = 0$ W, (c) transmittivity curve for $P_2 = 6.3$ W, (d) Xratio curve for $P_2 = 6.3$ W

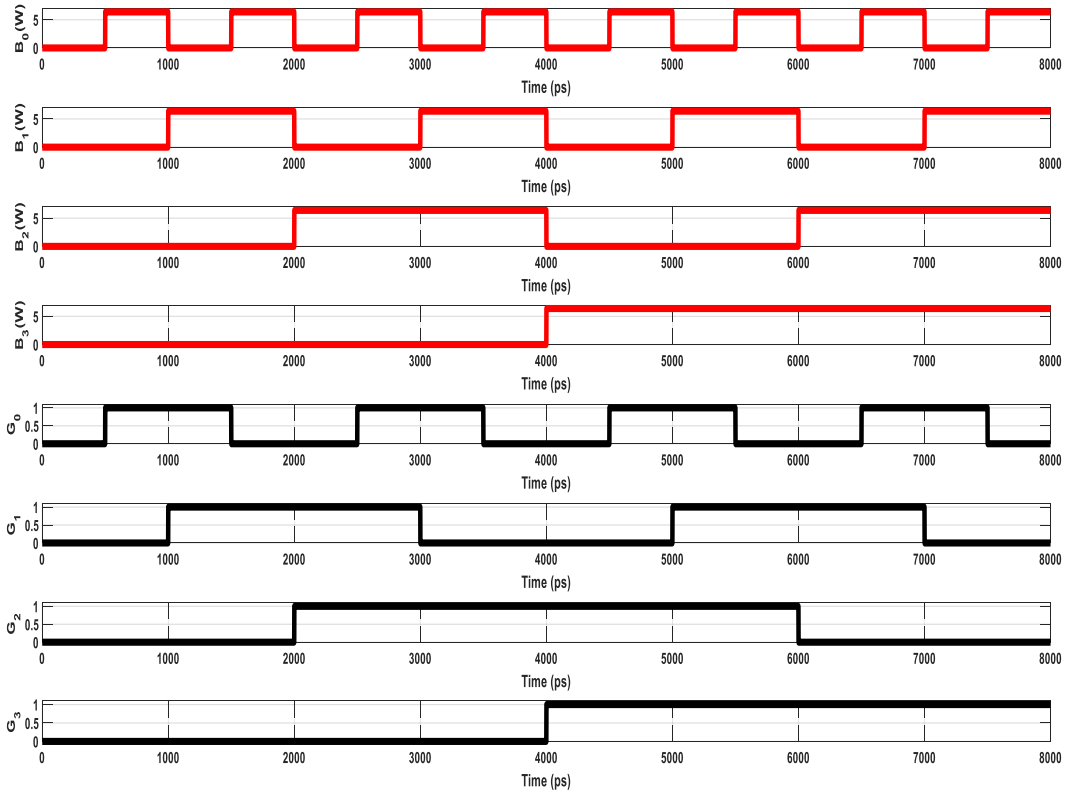

Fig. 7. Simulation result of the proposed all-optical 4-bit binary to gray code converter using XPM effect in directional couplers

5 All-optical even parity checker

A 4-bit all-optical even parity checker layout design is proposed using three XPM effect-based directional couplers as shown in Fig. 8. Each directional coupler generates the switching logic of XOR gate as shown in Fig. 2. The binary optical data bit patterns b_0 and b_1 are input to XOR1 with an output $C = b_1 \oplus b_0$. Similarly, the optical binary data b_2 and b_3 are input to XOR2 yielding an output $C = b_3 \oplus b_2$. Now, the output of XOR1 and XOR2 are sent to XOR3 through input ports A and B respectively. The output of XOR3 is the proposed 4-bit All-optical even parity checker which provides an optical pulse in the form of Boolean expression $P = (b_3 \oplus b_2) \oplus (b_1 \oplus b_0)$.

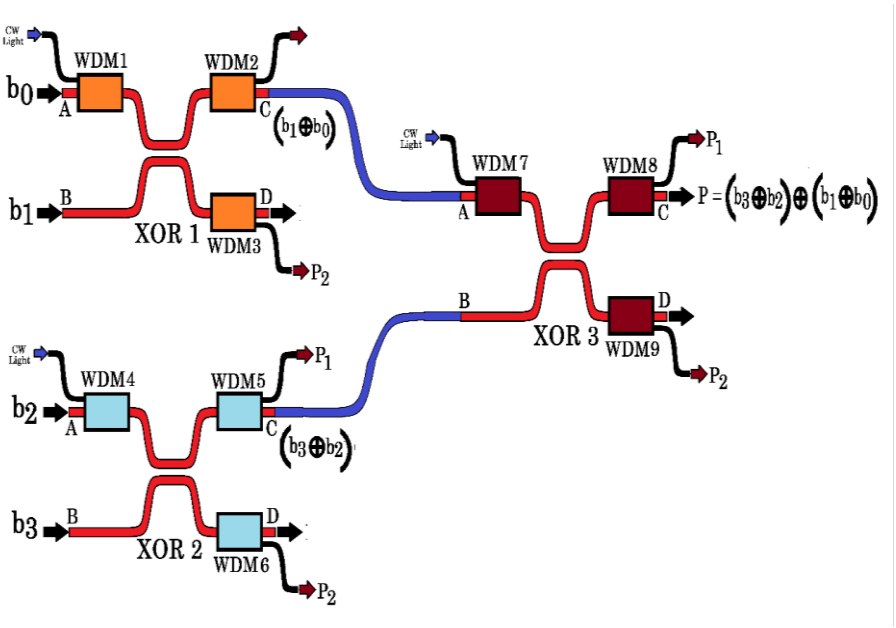

Fig. 8. Proposed layout design of 4-bit All-optical even parity checker using the XPM effect in directional couplers

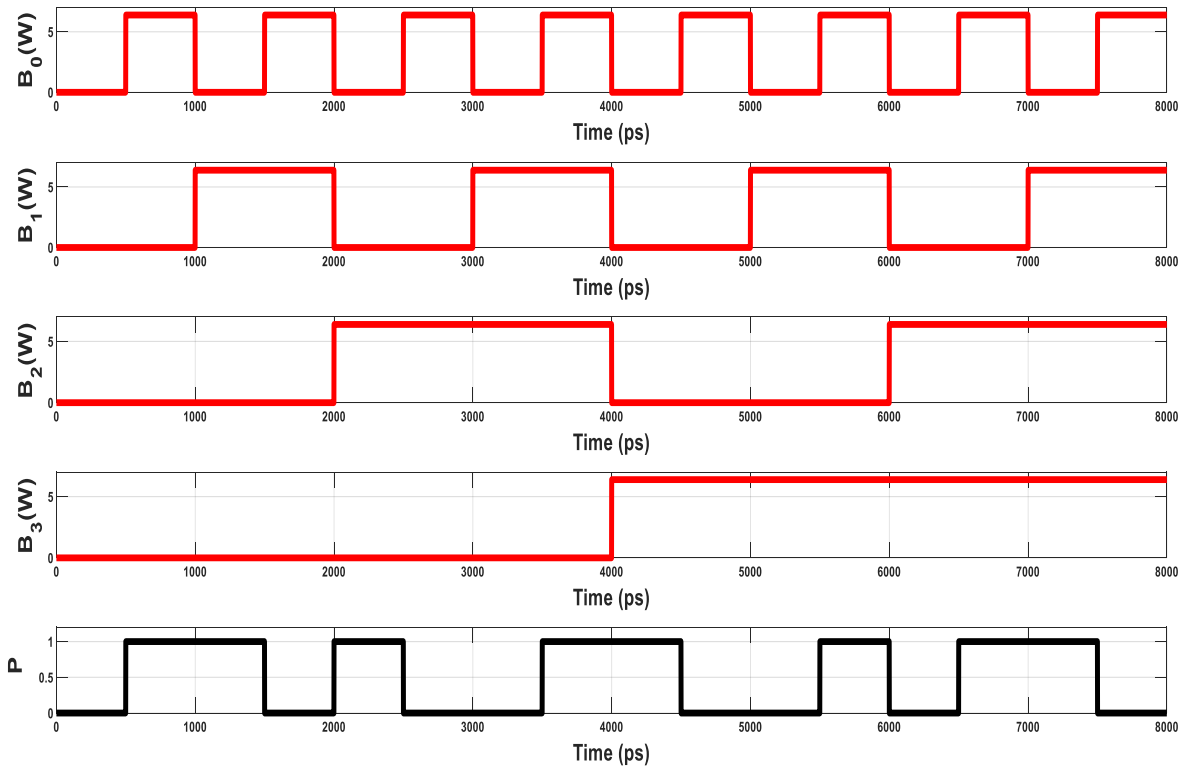

Fig. 9. Simulation result of the proposed 4-bit All-optical even parity checker using XPM effect in directional couplers

The proposed design of 4-bit All-optical even parity checker using the XPM effect is simulated, as shown in Fig. 9. Here, the 1st, 2nd, 3rd, and 4th row reveals the input optical binary data bit pattern $b_0, b_1, b_2,$ and b_3 respectively. The output of optical parity checker bit sequence is given in the 5th row. The input data bit pattern $b_0, b_1, b_2,$ and b_3 is simulated and the output is verified with the standard output of an even parity checker.

Therefore, the proposed device specifies an efficient approach where All-optical nonlinear directional couplers structure can be used for detection of an even number of 1's which can replace the conventional even parity checker circuit with All-optical circuits. Consequently, the implementation of 4-bit All-optical even parity checker using XPM effect in directional couplers can enhance the performance of switching.

6 Conclusion

In this paper, an efficient All-optical 4-bit binary to gray code converter and even parity checker using XPM effect based nonlinear directional coupler has been designed and simulated. The proposed 4-bit All-optical binary to gray code converter is designed using XOR logic gates, where the pump signal corresponding to logic (1) and (0) is 6.3 W and 0 W, respectively. The value of Xratio for (0,0) input setup is $\text{Xratio}_{12} = -340.4$ dB and $\text{Xratio}_{21} = 340.4$ dB. The suggested values show the perfect switching scenario for the proposed units. The optical switching action can be achieved if the input pump signal is greater than the threshold power. It is observed that, for input combination (0,1) and (1,0) the pump signal is greater than the suggested threshold power and the weak CW light is limited to the same core from which it was launched and for input combinations (0,1) and (1,0) the extinction ratio are $\text{Xratio}_{12} = 88.25$ dB and $\text{Xratio}_{21} = -88.25$ dB. On the other hand, for the input combinations (1,1) and (0, 0) the extinction ratio are $\text{Xratio}_{12} = -340.3$ dB and $\text{Xratio}_{21} = 340.3$ dB. Consequently, the represented data signifies that the selected pump power levels are appropriate for the perfect All-optical XOR functionality. Further, the optimized number of All-optical XOR logic gates are used to design the layouts of the proposed 4-bit All-optical binary to gray code converter and even parity checker. Finally, the designed methodology is verified using the proper simulation results and it may be useful in order to design optimized low power switching activity for high speed, fast switching, and decision-making optical units.

References

[1] H. Han, M. Zhang, P. Ye, and F. Zhang, "Parameter design and performance analysis of an ultrafast all-optical XOR gate based on quantum dot semiconductor optical amplifiers in nonlinear Mach-Zehnder interferometer," *Opt. Commun.*, vol. 281, pp. 5140–5145, 2008.

[2] J. K. Rakshit, K. E. Zoiros, and G. K. Bharti, "Proposal for ultrafast all-optical pseudo-random binary sequence generator using microring resonator-based switches," *J. Comput. Electron.*, vol. 20, pp. 353–367, 2021.

[3] Z. Pan, P. Lang, and G. Duan, "An all-optical switch based on a surface plasmon polariton resonator," *Mod. Phys. Lett. B*, vol. 32, p. 1850134, 2018.

[4] Q. Li et al., "All-optical logic gates based on cross-phase modulation effect in a phase-shifted grating," *Appl. Opt.*, vol. 55, p. 6880, 2016.

[5] S. Masilamani and P. Samundiswary, "Compact and efficient PC-based directional coupler all-optical switch," *J. Opt. Commun.*, 2020.

[6] E. G. Anagha and R. K. Jeyachitra, "Investigations on All-Optical Binary to Gray and Gray to Binary Code Converters Using 2D Photonic Crystals," *IEEE J. Quantum Electron.*, vol. 57, 2021.

[7] M. J. Potasek and Y. Yang, "Multiterabit-per-second All-Optical Switching in a Nonlinear Directional Coupler," IEEE J. Sel. Top. *Quantum Electron.*, vol. 8, no. 3, 2002.

[8] W. B. Fraga, J. W. M. Menezes, M. G. da Silva, C. S. Sobrinho, and A. S. B. Sombra, "All optical logic gates based on an asymmetric nonlinear directional coupler," *Opt Commun*, vol. 262, no. 1, pp. 32–37, Jun. 2006.

[9] J. S. de Almeida et al., "Logic gates based in asymmetric couplers: Numerical analysis," *Fiber Integr. Opt.*, vol. 26, pp. 217–228, 2007.

[10] Q. Li, A. Zhang, and X. Hua, "Numerical simulation of solitons switching and propagating in asymmetric directional couplers," *Opt Commun*, vol. 285, no. 2, pp. 118–123, Jan. 2012.

[11] Q. Li, Z. Zhang, S. Li, M. Hu, Y. Wei, and Y. Lu, "All-optical logic gates based on wavelength conversion in a nonlinear directional coupler," *Opt Commun*, vol. 354, pp. 246–249, Jun. 2015.

[12] S. R. Friberg, A. M. Weiner, Y. Silberberg, B. G. Sfez, and P. S. Smith, "Femtosecond switching in a dual-core-fiber nonlinear coupler," *Opt. Lett.*, vol. 13, 1988.

[13] Z. Farrokhi Chaykandi, A. Bahrami, and S. Mohammadnejad, "MMI-based all-optical multi-input XOR and XNOR logic gates using nonlinear directional coupler," *Opt. Quantum Electron.*, vol. 47, pp. 3477–3489, 2015.

[14] J. Wilson, G. I. Stegeman, and E. M. Wright, "Soliton switching in an erbium-doped nonlinear fiber coupler," vol. 16, 1991.

[15] X. He, K. Xie, and A. Xiang, "Optical solitons switching in asymmetric dual-core nonlinear fiber couplers," *Optik*, vol. 122, pp. 1222–1224, 2011.

[16] A. Ghadi and S. Mirzanejhad, "All-optical logic gates using semiconductor-based three-coupled waveguides nonlinear directional coupler," *Opt. Commun.*, vol. 284, pp. 432–435, 2011.

[17] H. Sharifi, S. M. Hamidi, and K. Navi, "All-optical photonic crystal logic gates using nonlinear directional coupler," *Photonics Nanostruct.*, vol. 27, pp. 55–63, 2017.

[18] A. Yadav, A. Kumar, and A. Prakash, "Design and analysis of all-optical half and full adder/subtractor using nonlinear asymmetric directional couplers," *Optik*, vol. 288, p. 171190, Oct. 2023, doi: 10.1016/j.ijleo.2023.171190.

[19] P. Mandal and S. Midda, "All optical method of developing or and NAND logic system based on nonlinear optical fiber couplers," *Optik*, vol. 122, pp. 1795–1798, 2011.

[20] A. G. Coelho et al., "Switching and enhanced bistability in an asymmetric nonlinear directional coupler with a metamaterial channel," *Commun. Nonlinear Sci. Numer. Simul.*, vol. 18, pp. 1258–1268, 2013.

[21] M. I. Asjad et al., "The fractional comparative study of the non-linear directional couplers in non-linear optics," *Results Phys.*, vol. 27, 2021.

[22] X. He, "Phase-induced switching in fiber nonlinear directional coupler," *Optik*, vol. 125, pp. 2267–2269, 2014.

Received 24 October 2023